forests

Article

Changes in Soil Physical and Chemical Properties during Vegetation Succession on Miyake-jima Island

Xinhao Peng, Kenji Tamura *, Maki Asano, Aya Takano, Minami Kawagoe and Takashi Kamijo

Graduate School of Life and Environmental Sciences, University of Tsukuba, Tsukuba 305-8572, Japan; pengxh92@gmail.com (X.P.); asano.maki.fw@u.tsukuba.ac.jp (M.A.); seal-10201.atlan@i.softbank.jp (A.T.); maru3705@yahoo.co.jp (M.K.); kamijo.takashi.fw@u.tsukuba.ac.jp (T.K.)
* Correspondence: tamura.kenji.gn@u.tsukuba.ac.jp; Tel.: +81-29-853-7201

Abstract: The bare lands formed after volcanic eruptions provide an excellent opportunity to study the interactions between vegetation succession and soil formation. To explore the changes in soil physicochemical properties in the vegetation succession processes and the relationship between them, soil physicochemical properties of different volcanic ash accumulation on Miyake-jima Island were studied at different vegetation succession stages. The results showed that soil bulk density gradually decreased and that soil porosity, soil water content (SWC), pH, cation exchange capacity (CEC), soil total organic carbon (*TOC*), and total nitrogen (TN) increased significantly with vegetation succession. The physicochemical properties changes in the soil surface horizon were most obvious, and the deep soil accumulated a large amount of relatively stable soil carbon and nitrogen. The forest land formed a thicker organic matter horizon, accumulating more carbon and nitrogen than grassland, and the soil quality index (*SQI*) was higher than that of grassland and shrubland. In conclusion, our research indicates the significant change in soil physicochemical properties and the improvement in soil quality in the vegetation succession processes, emphasizing a significant relationship between vegetation succession and soil development in bare land.

Keywords: vegetation succession; soil bulk density; soil porosity; soil organic carbon; volcanic island

Citation: Peng, X.; Tamura, K.; Asano, M.; Takano, A.; Kawagoe, M.; Kamijo, T. Changes in Soil Physical and Chemical Properties during Vegetation Succession on Miyake-jima Island. *Forests* **2021**, *12*, 1435. https://doi.org/10.3390/f12111435

Received: 12 August 2021
Accepted: 19 October 2021
Published: 21 October 2021

Publisher's Note: MDPI stays neutral with regard to jurisdictional claims in published maps and institutional affiliations.

1. Introduction

Physical and chemical weathering play a key role in soil formation. The weathering products of parent materials provide the necessary nutrient elements for plant development and growth [1,2], regulate the chemical composition of soil [3,4] and groundwater [5,6], and gradually transform parent materials into soil suitable for vegetation growth. At the same time, vegetation plays an important role in controlling the formation of soil [7–9]. In general, vegetation accelerates soil formation by promoting physical and chemical weathering of parent materials. For example, the roots of vegetation accelerate the physical disintegration of parent materials [10], change their exposed surface area [11,12], and form organic chelates, which further accelerate the weathering of parent materials after disintegration due to the large numbers of root exudates, such as organic acids and ligands [12]. In addition, vegetation canopies have the functions of intercepting rainfall and reducing soil water evaporation. In addition, combined with the soil pore structures produced by roots, they deepen the infiltration capacity of soil and the vertical preferential flow, further increase the soil water residence time and soil solute flux, and create favorable weathering conditions. At the same time, they in turn promote vegetation growth. Chadwick et al. [8] used chrono sequences along with an altitudinal gradient in Hawaii to emphasize the importance of soil moisture and the physical properties of soil in controlling water percolation, cation leaching, and soil formation.

Volcanic soils account for only 0.8 percent of the world's land area, but they store up to 5 percent of the global soil carbon (C) pool [13]. The volcanic soils (Andisols) formed after volcanic eruptions are among the most fertile lands for cultivation in the world. Nearly

60 volcanoes erupt around the world every year. The high-temperature magma and forest fires caused by volcanoes destroy vegetation, form a large area of bare land, and force vegetation succession, thus providing unique conditions for studying vegetation succession, especially in the early stages of primary succession [14]. Pyroclastic and associated soil cover more than 124 million hectares of the earth's surface [15], and the major areas of these volcanic areas are along the Pacific Rim, where oceanic plate subductions produce extensive rhyolitic and andesitic volcanism. The weathering and development of volcanic ash soils show similar patterns in different parts of the world. In temperate and tropical environments with sufficient rainfall, volcanic sediments usually form volcanic soil with sufficient moisture under weathering [16].

Miyake-jima Island is a stratovolcano composed of basalt with a circular area of 55.44 km^2 in Japan. In the last 100 years, volcanic eruptions were observed in 1940, 1962, 1983, and 2000 [17]. Although the basic composition of volcanic ash is basalt, the accumulated volcanic ash showed strong acidity due to the release of volcanic gas, dissolved a large amount of aluminum and calcium in the form of sulfate, and gradually formed a hard crust, which led to a relatively poor living environment for the growth of vegetation [17]. According to a chrono sequence study on the lava flow of different ages, the primary succession process on Miyake-jima Island can be summarized as follows: (1) the successful colonization of pioneer species, such as deciduous *Alnus sieboldiana* (a N-fixing tree), *Miscanthus condensatus* (a perennial grass), and *Fallopia japonica* var. *hachidyoensis* (a perennial herb), on bare lava flows; (2) the colonization of seral deciduous species, such as *Prunus speciosa*, and climax evergreen species, such as *Machilus thunbergii* and *Castanopsis sieboldii*; and (3) the establishment of climax forests composed of evergreen *C. sieboldii* [18]. In 2000, after 18 years, Miyake-jima Island erupted again, and the representative vegetation of the island suffered a devastating disaster. Before the eruption in 2000, the eruptions of Miyake-jima Island in 1874, 1940, 1962, and 1983 were of a fissure vent type, and they were accompanied by lava and scoria eruptions [19,20]. However, the eruption in 2000 was completely different in regard to the fissure vent type, where a caldera was formed, and a large amount of volcanic ash was emitted at the same time. In addition, a large amount of volcanic gas containing high concentrations of sulfur dioxide was released for a long time. Especially on the slopes above 300 m above sea level, 96% of the vegetation (1700 ha) disappeared within two months after the eruption, while the volcanic ash produced during the eruption accumulated on the hillside [21,22]. As a characteristic of volcanic activity, the long-term release of volcanic gas caused long-term vegetation disasters on the hillside and led to surface acidification [23–25]. According to observations of the released sulfur dioxide (one of the main components of volcanic gas), although the release tended to decrease gradually, the released volcanic gas still caused leaf death 7 years after the volcanic eruption [26]. The chemical composition of volcanic ash was basaltic as before, but it contained more clay and higher base saturation, which made its properties very different [17]. Due to the surface acidification, primary minerals, such as plagioclase and volcanic glass, as well as the dissolution of some smectites, released a large amount of aluminum. The harsh soil environment caused by this volcanic eruption was gradually improved with vegetation restoration.

The bare land vegetation succession formed by the volcanic eruption of Miyake-jima Island in 2000 provides a unique opportunity to understand soil development and vegetation restoration after volcanic eruptions. The objectives of this paper are to investigate (1) the changes in the soil properties, such as soil porosity and soil bulk density, during vegetation succession processes, (2) the differences in the soil properties at different vegetation succession stages, and (3) the effects of volcanic ash deposition on the geomorphology and soil properties of Miyake-jima Island.

2. Materials and Methods

2.1. Study Site

Miyake-jima Island (34°04′37″ N, 139°31′34″ E) is located in the sea of Sagami Bay, approximately 180 km southeast of Tokyo, Japan. The annual average temperature is 17.4 °C, and the annual precipitation is 2872 mm [27]. The island has a humid subtropical climate with hot summer, warm winter, and abundant precipitation throughout the year. The warm and wet flow from the tropics creates warm and moist conditions in summer [28].

The Igaya area in the west of Miyake-jima Island was selected, and three research sites (IG7, IG8, and IG9) with different elevation gradients along the ridge were set up (Figure 1). All sites were developed from the same parent materials and were covered by vegetation at different succession stages. Before 2000, IG7, IG8, and IG9 were covered with *Eurya japonica var. japonica*, *Castanopsis sieboldii*, and *Cryptomeria japonica*, respectively. Satellite images confirm that all research sites (IG7, IG8, IG9) completely lost the vegetation following the 2000 eruption. They were also covered by volcanic ash and were less affected by volcanic gas [29]. Now the IG7 is covered by the vegetation type of grassland. This vegetation type comprises the following dominant species: *Miscanthus condensatus*, *Fallopia japonica*, *Calamagrostis autumnalis*, and *Carex okuboi*. The IG8, which has become shrubland, is mainly composed of the following species: *Alnus sieboldiana* (small size trees), *Rubus trifidus*, *Dryopteris caudipinna*, and *Miscanthus condensatus*. The vegetation type of forest land covers the IG9 at the lowest altitude. This vegetation type comprises the following dominant species: *Alnus sieboldiana*, *Kadsura japonica*, *Dryopteris caudipinna*, *Trachelospermum asiaticum*, and *Rubus trifidus* (Table 1).

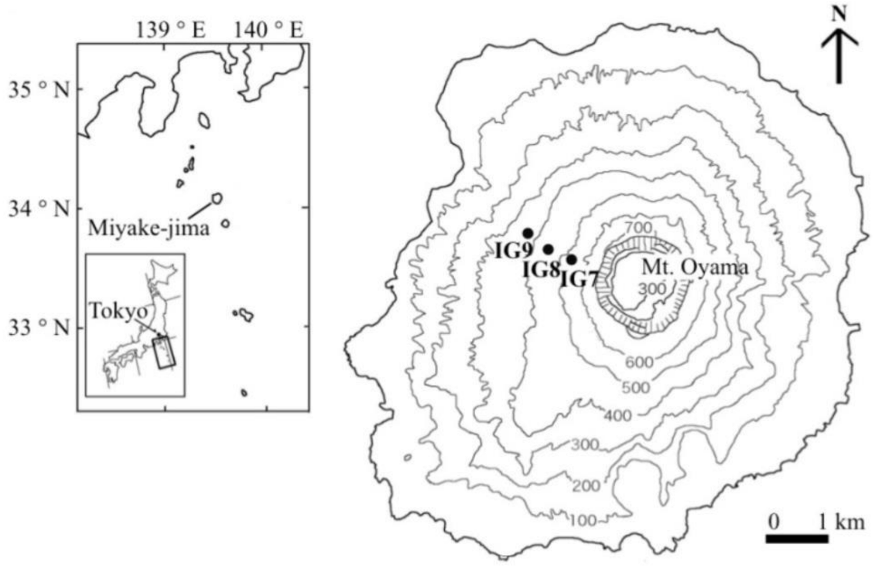

Figure 1. Location of the study sites on Miyake-jima Island.

2.2. Soil Sampling

Field investigations were carried out at the locations of the three research sites in December 2007, December 2011, and October 2019, respectively. After the litter on the ground was removed, the soil profile was investigated according to the soil survey manual of the Japanese Society of Pedology, and the profile description included soil color, texture, structure, and root in the wet state. The soil survey manual refers to soil classification guidelines such as the Unified Soil Classification System of Japan, Soil Description (FAO), Soil Taxonomy (USDA), and so on [30]. A stainless cutting ring with a diameter of 50 mm and a height of 51 mm (Daiki, DIK-180) was used to collect soil bulk samples of 0–5 cm, 10–15 cm, 30–35 cm, 50–55 cm, and 70–75 cm from top to bottom, with 3 repeats in each horizon. At the same time, three replicate representative bulk soil samples were collected from each soil horizon of each site.

Table 1. Geographical and vegetation characteristics of the three study sites.

Site	Altitude (m)	Aspect (°)	Slope (°)	Volcanic Ash Thickness (cm)	Vegetation Restoration Time	Land Cover Types	Coverage (%)	Main Plant Species
IG7	538	N50W	6	43	7	Bare land	<1	—
					11	Grassland	55	*Miscanthus condensatus*
					19	Grassland	99	*Miscanthus condensatus*
IG8	443	N60W	12	38	7	Grassland	91	*Miscanthus condensatus*
					11	Shrubland	130	*Rubus trifidus*
					19	Shrubland	176	*Alnus sieboldiana*
IG9	388	N50W	6	20	7	Shrubland	131	*Alnus sieboldiana*
					11	Forest land	180	*Alnus sieboldiana*
					19	Forest land	242	*Alnus sieboldiana*

Coverage is the total vegetation coverage of the tree, shrub, and herb horizons.

2.3. Laboratory Procedures

The actual volume of the sample in the soil cutting ring was measured using a digital actual volumenometer (Daiki, DIK-1150, Kounosu, Japan). The bottom of the cutting ring was immersed in degassed water for 24 h to weigh the saturated weight after achieving capillary saturation and then the drying weight after drying in an oven at 105 °C for 24 h. The three-phase distribution of the soil was calculated, and its hydraulic conductivity was measured by distilled water using the constant water head method (Daiki, DIK-4050, Kounosu, Japan). After all the bulk soil samples were air-dried for 2 months and gently crushed to pass 2-mm and 0.5-mm sieves, the roots and stones were removed to determine the physical and chemical properties of the soil. The soil pH was determined in both deionized water and 1N KCl in a 1:2 soil-to-solution ratio using a glass electrode. The cation exchange capacity (CEC) was determined using the ammonium acetate method of Schollenberger [31]. The total organic carbon (*TOC*) and total nitrogen (TN) contents were determined using dry combustion on an NC Analyzer (Sumika Chemical Analysis Service, SUMIGRAPH NC 220F, Osaka, Japan).

2.4. Evaluation of Soil Quality Index

Principal component analysis (PCA) and Pearson's correlation analysis were used to screen the best representative soil indicators by using SPSS 27.0 (SPSS Inc., Chicago, IL, USA). If the indicators were well correlated (correlation coefficient > 0.6) with each other, only the highest weighted indicator was retained in the PC. A nonlinear scoring function was performed to transform the representative soil indicators into scores of 0 to 1 [32] (Equation (1)). Finally, a formula was used to calculate soil quality index (*SQI*) to assess soil quality [33] (Equation (2)).

$$S = a/\left(1 + (x/x_0)^b\right) \tag{1}$$

where S is the score of soil indicator, a reflects the maximum value reached by the function (a = 1), x is the value of the indicator, x_0 is mean value of each soil indicator, and b is the value of the equation's slope. Using $b = -2.5$, the value provided curves that vary between 0 and 1 in a suitable way [34,35].

$$SQI = \sum_{i=1}^{n} S_i * W_i \tag{2}$$

where W_i is the weighting values of the representative soil indicators determined by PCA, n is the number of the representative soil indicators. One-way analysis of variance (ANOVA) followed by least-significant difference (LSD) was used to examine and to compare the differences in soil indicators and *SQI* among different soil horizons at $p < 0.05$ level [36].

3. Results

3.1. Morphological Features of the Soil Profiles

Due to the frequent eruption of Miyake-jima Island, the ash thicknesses of the three study sites, which were at different altitudes on the ridge, were different. After the eruption in 2000, the ash accumulation thicknesses of IG7, IG8, and IG9 were 43 cm, 38 cm, and 20 cm, respectively. The depth of the 2A horizon, which was formed by the three sites after the 1983 eruption, was different. The 2A horizon of IG7, which is closest to the crater and has the highest altitude, was deepest. Due to the island being formed by volcanic eruptions, the soil had a very significant active aluminum reaction with a stronger aluminum reaction on the soil surface, which is consistent with the high degree of weathering on the soil surface and the leaching of a large amount of active aluminum. In our study (Table S1), all the soils had black (2.5Y 2/1) to dark brown (2.5Y 3/1) fragile loam and clay soil except for the deeper part of the C horizon, which had sandy soil with little stones. All the sites had crumb or subangular blocky A/B horizons with slightly sticky plastic and a massive C horizon without sticky plastic. The soil hardness increased with the depth, resulting in the number of roots gradually decreasing until they disappeared.

In the 2007 survey, there was no A horizon at each site, and no soil structure development was observed in the surface horizons (Figure S1). In the 2011 survey, a slight formation of the A horizon was observed in IG9. Furthermore, in 2019, a crumb structure was observed on the surface horizon at each site, and an A horizon was confirmed. The development of the A horizon only took place 20 years after the 2000 eruption, which is a characteristic result of this study.

3.2. Three-Phase Distribution and Hydraulic Conductivity of the Soil Core Samples

In 2019, the solid fraction of the surface soil in the accumulation horizon after the volcanic eruption in 2000 was lower, but it gradually increased with the depth. Furthermore, the buried horizon, which is the accumulation before the volcanic eruption in 2000, also had a lower solid fraction. Compared with the sites of the three different succession stages, the surface horizon of IG7 had the highest solid and gas fractions and the lowest liquid fraction, while the surface horizon of IG9 covered by tree vegetation had the highest liquid fraction. In the same soil profile, the soil hydraulic conductivity of the A horizon (0–5 cm) and C3 horizon (30–35 cm) of IG7 was higher and was 0.12 and 0.19 cm/s, respectively. The 3C horizon (50–55 cm) of IG8 was higher, and it was 0.22 cm/s, and those of the A horizon (0–5 cm), Cd horizon (10–15 cm), and 3C horizon (30–35 cm) of IG9 were higher, and they were 0.06, 0.06, and 0.11 cm/s, respectively (Table 2).

3.3. Bulk Density

Similar to the change in porosity, the soil bulk density significantly increased with depth and decreased with time ($p < 0.05$; Figure 2), while the deep soil bulk density even slightly increased. In 2019, the surface bulk density of IG7, IG8, and IG9 was 1.19 g/mL, 0.81 g/mL, and 0.89 g/mL, respectively. In comparison, the soil bulk density of IG7 near the crater was highest, indicating that the degree of weathering in the grassland was weaker than that in the forest land (Table 2).

3.4. Soil Porosity

In the soil formed by the accumulation of the volcanic ash from the same volcanic eruption, the total soil porosity decreased with depth and increased with vegetation succession, indicating that the soil gradually weathered with the vegetation growth. Moreover, the internal porosity of the soil gradually increased, and the weathering degree of the surface soil was highest ($p < 0.05$; Figure 3). In the deep soil formed by the accumulated volcanic ash after the volcanic eruption in 2000, the total soil porosity even slightly decreased due to the lack of weathering conditions. The change in the soil capillary porosity was similar to that of the total porosity, and the increase in the surface soil capillary porosity with time was particularly significant, indicating that the aeration and water storage capacity of the island's surface soil were gradually increasing ($p < 0.05$; Figure 3). At the same time, the capillary porosity of IG9 was highest among the three sites, indicating that the forest land had better soil weathering conditions, which is consistent with the three-phase distribution.

Table 2. Three-phase distribution, soil porosity, and hydraulic conductivity of different sites in 2019 (means and standard error).

Depth (cm)	Three-Phase Distribution (%)			Soil Porosity (%)			Hydraulic Conductivity (cm/s)
	Solid Fraction	Liquid Fraction	Gas Fraction	Total Porosity	Capillary Porosity	Non-Capillary Porosity	
IG7							
0–5	39.5 (0.4)	26.6 (1.1)	34.0 (0.7)	60.5 (0.4)	52.5 (0.9)	8.0 (0.8)	11.7×10^{-2} (0.0002)
10–15	44.7 (2.4)	36.2 (1.0)	19.2 (1.5)	55.3 (2.4)	47.1 (1.4)	8.2 (1.2)	0.6×10^{-2} (0.003)
30–35	44.7 (1.6)	19.6 (0.5)	35.6 (2.1)	55.3 (1.6)	46.3 (0.9)	9.0 (0.9)	18.9×10^{-2} (0.01)
50–55	27.4 (1.0)	66.9 (2.0)	5.7 (1.1)	72.6 (1.0)	71.2 (1.2)	1.4 (0.2)	0.1×10^{-2} (0.0002)
70–75	29.3 (1.4)	63.4 (2.2)	7.3 (1.0)	70.7 (1.4)	66.5 (2.0)	4.2 (0.8)	0.1×10^{-2} (0.0002)
Mean *	37.1 (1.4) ^{a}	42.5 (1.4) ^{a}	20.4 (1.3) ^{a}	62.9 (1.4) ^{a}	56.7 (1.3) ^{a}	6.2 (0.8) ^{a}	6.3×10^{-2} (0.003) ^{a}
IG8							
0–5	31.3 (3.1)	46.3 (1.6)	22.4 (2.7)	68.7 (3.1)	60.5 (0.6)	8.2 (2.8)	0.1×10^{-2} (0.0005)
10–15	43.6 (1.2)	44.9 (0.6)	11.6 (1.7)	56.4 (1.2)	50.9 (0.4)	5.5 (0.8)	0.1×10^{-2} (0.0005)
30–35	42.3 (1.2)	36.2 (2.4)	21.6 (1.4)	57.7 (1.2)	50.8 (1.0)	7.0 (0.7)	0.1×10^{-2} (0.0008)
50–55	30.2 (2.5)	22.7 (0.8)	47.0 (3.3)	69.8 (2.5)	54.4 (2.2)	15.4 (0.4)	21.6×10^{-2} (0.01)
70–75	46.1 (1.1)	33.0 (2.6)	21.0 (2.1)	53.9 (1.1)	38.0 (2.5)	15.9 (2.0)	0.1×10^{-2} (0.0001)
Mean *	38.7 (1.8) ^{a}	36.6 (1.6) ^{b}	24.7 (2.3) ^{a}	61.3 (1.8) ^{a}	50.9 (1.3) ^{b}	10.4 (1.3) ^{b}	4.4×10^{-2} (0.0003) ^{a}
IG9							
0–5	32.9 (3.6)	52.5 (1.6)	14.6 (4.4)	67.1 (3.6)	62.6 (2.1)	4.5 (2.6)	6.1×10^{-2} (0.05)
10–15	43.2 (3.0)	30.3 (2.2)	26.6 (3.7)	56.8 (3.0)	49.6 (3.4)	7.2 (1.0)	6.1×10^{-2} (0.05)
30–35	26.4 (1.7)	37.9 (4.3)	35.7 (4.3)	73.6 (1.7)	59.0 (1.9)	14.6 (1.0)	11.2×10^{-2} (0.05)
50–55	30.8 (2.0)	49.7 (1.1)	19.5 (2.3)	69.2 (2.0)	60.9 (1.7)	8.3 (0.5)	0.8×10^{-2} (0.006)
70–75	41.8 (1.9)	41.0 (2.7)	17.2 (1.9)	58.2 (1.9)	46.9 (2.2)	11.4 (0.7)	0.1×10^{-2} (0.0001)
Mean *	35.0 (2.4) ^{a}	42.3 (2.4) ^{a}	22.7 (3.3) ^{a}	64.9 (2.4) ^{a}	55.8 (2.3) ^{a}	9.2 (1.1) ^{b}	4.8×10^{-2} (0.03) ^{a}

* Different letters express significant difference within the column; one-way ANOVA, $p < 0.05$.

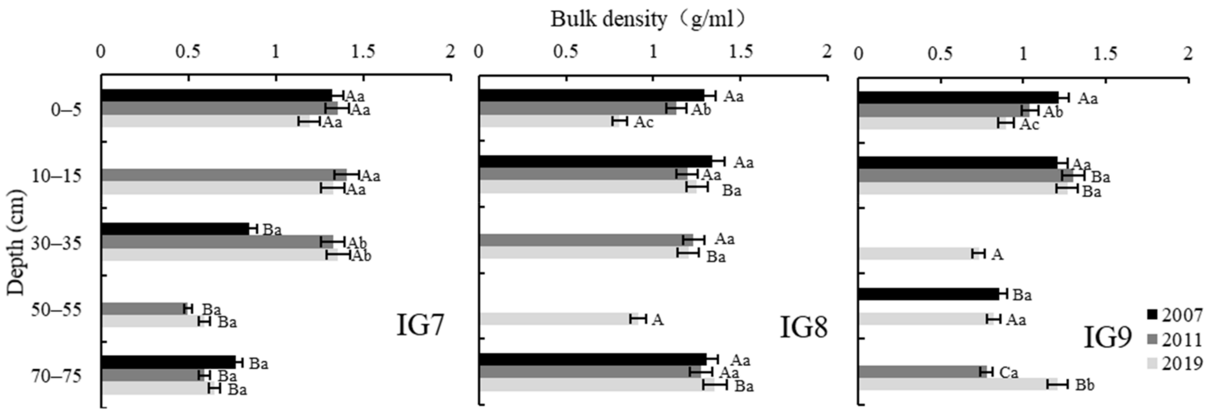

Figure 2. Bulk density at the different sites; different lowercase letters express significant difference at the same depth (one-way ANOVA, $p < 0.05$), and different uppercase letters express significant difference under different soil depths (one-way ANOVA, $p < 0.05$).

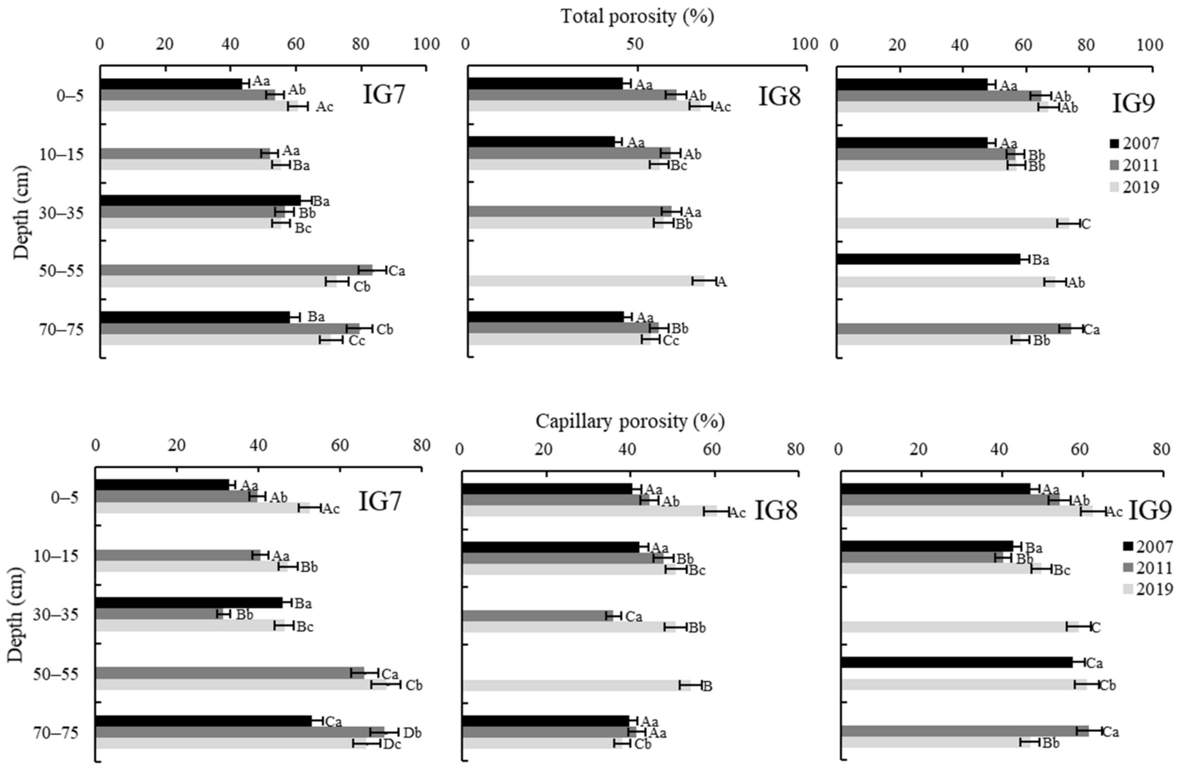

Figure 3. Total porosity and capillary porosity at the different sites; different lowercase letters express significant difference at the same depth (one-way ANOVA, $p < 0.05$), and different uppercase letters express significant difference under different soil depths (one-way ANOVA, $p < 0.05$).

3.5. pH and Cation Exchange Capacity

In the early succession stage, the soil pH maintained a consistent low value in 2007, the pH in the surface soil was highest, and the soil pH gradually tended toward neutral with vegetation succession ($p < 0.05$; Table 3). With the gradual vegetation growth, the CEC content showed a gradually increasing trend. In 2019, the CEC content in the surface horizons of IG7, IG8, and IG9 was 4.76 cmol/kg, 12.28 cmol/kg, and 19.36 cmol/kg, respectively. For the soil accumulated by the volcanic eruption in 2000, the CEC content of IG7 in 2019 was 4.76–6.91 cmol/kg, while the CEC content in deep soil was 7.92–18.63 cmol/kg. Soil formed before the volcanic eruption in 2000 had a higher CEC content, as shown in Table 3.

3.6. Total Organic Carbon Contents and Total Nitrogen Contents

For the accumulated volcanic ash soil after the volcanic eruption in 2000, the *TOC* content of IG7 in 2007, 2011, and 2019 was 1.26 g/kg, 0.76–1.31 g/kg, and 1.29–8.04 g, respectively, and the *TOC* content of IG8 was 4.44–21.94 g/kg, 0.35–11.10 g/kg, and 1.47–38.02 g/kg, respectively. The *TOC* content of IG9 was 0.18 g/kg, 1.70–58.53 g/kg, and 11.12–47.84 g/kg, respectively (Table 4). The soil *TOC* significantly increased with time and decreased with the increase in altitude ($p < 0.05$; Table 4). The volcanic ash accumulation thickness was large in the area close to the crater, and the contribution of the growing herbaceous vegetation to the soil carbon accumulation was low. However, the *TOC* content in the deep soil of IG7 was 4.87–70.62 g/kg, which resulted in the storage of a large amount of soil carbon in the depths of the ground due to the frequent eruption of Miyake-jima Island.

Table 3. pH and cation exchange capacity (CEC) at different sites (means and standard error).

Sites	pH (H_2O)			pH (KCl)			CEC (cmol/kg)		
	2007	2011	2019	2007	2011	2019	2007	2011	2019
IG7									
A/C1d	3.9 (0.03)	4.8 (0.03)	5.7 (0.03)	3.8 (0.01)	4.1 (0.03)	4.7 (0.01)	4.6 (0.11)	6.7 (0.17)	4.8 (0.10)
C1d	3.9 (0.02)	4.8 (0.04)	5.9 (0.02)	3.8 (0.03)	4.1 (0.02)	4.8 (0.02)	4.6 (0.13)	6.7 (0.12)	6.9 (0.24)
C2d	3.9 (0.04)	4.3 (0.02)	5.5 (0.01)	3.8 (0.02)	4.0 (0.02)	4.4 (0.03)	4.6 (0.28)	5.5 (0.18)	6.9 (0.06)
C3	3.9 (0.04)	4.3 (0.03)	5.2 (0.02)	3.8 (0.02)	4.0 (0.02)	4.3 (0.01)	4.6 (0.19)	5.5 (0.13)	5.4 (0.09)
C4	3.9 (0.02)	4.4 (0.03)	5.1 (0.02)	3.8 (0.02)	4.1 (0.02)	4.3 (0.01)	3.5 (0.29)	4.6 (0.26)	6.9 (0.11)
2A1	3.9 (0.03)	4.4 (0.02)	5.2 (0.01)	4.0 (0.02)	4.1 (0.02)	4.6 (0.01)	16.7 (0.21)	23.5 (0.19)	18.6 (0.13)
2A2	3.9 (0.03)	4.6 (0.02)	4.9 (0.01)	4.1 (0.01)	4.4 (0.03)	4.7 (0.01)	9.5 (0.21)	12.2 (0.25)	15.1 (0.14)
$2B_W$	3.9 (0.02)	4.6 (0.04)	4.7 (0.01)	4.1 (0.03)	4.5 (0.02)	4.7 (0.01)	7.9 (0.25)	11.7 (0.13)	16.9 (0.08)
3C	4.0 (0.03)	4.6 (0.03)	4.7 (0.01)	4.4 (0.02)	4.7 (0.03)	4.8 (0.01)	1.3 (0.23)	1.0 (0.14)	7.9 (0.27)
Mean *	3.9 (0.03) ^{Aa}	4.4 (0.03) ^{Ab}	5.1 (0.02) ^{Ac}	3.9(0.02) ^{Aa}	4.2 (0.02) ^{Aa}	4.5 (0.01) ^{Ab}	6.1 (0.21) ^{Aa}	8.2 (0.17) ^{Ab}	10.2 (0.14) ^{Ac}
IG8									
A/C1d	3.9 (0.03)	4.6 (0.04)	5.3 (0.03)	3.6 (0.01)	4.2 (0.02)	4.3 (0.01)	6.4 (0.18)	8.2 (0.11)	12.3 (0.01)
C1d	4.1 (0.02)	4.8 (0.02)	5.7 (0.01)	3.8 (0.03)	4.2 (0.01)	4.5 (0.01)	7.1 (0.22)	9.2 (0.15)	8.5 (0.05)
C2	3.8 (0.03)	4.6 (0.02)	5.0 (0.02)	3.7 (0.02)	4.1 (0.03)	4.3 (0.01)	8.0 (0.19)	7.7 (0.16)	5.9 (0.07)
2A	4.1 (0.02)	4.7 (0.04)	5.0 (0.01)	4.1 (0.02)	4.3 (0.03)	4.5 (0.02)	15.4 (0.11)	20.5 (0.21)	17.6 (0.16)
3C	3.8 (0.02)	4.7 (0.02)	5.1 (0.01)	4.2 (0.01)	4.5 (0.02)	4.8 (0.01)	-	6.0 (0.24)	8.2 (0.17)
4B	4.0 (0.02)	4.7 (0.03)	4.8 (0.02)	4.3 (0.01)	4.5 (0.02)	4.8 (0.01)	10.8 (0.12)	9.6 (0.18)	3.9 (0.23)
5C	4.2 (0.02)	4.8 (0.03)	5.0 (0.02)	4.6 (0.02)	4.7 (0.02)	5.0 (0.01)	1.0 (0.11)	3.8 (0.17)	3.7 (0.11)
Mean *	4.1 (0.02) ^{Aa}	4.7 (0.03) ^{Ab}	5.1 (0.02) ^{Ac}	4.1 (0.02) ^{Aa}	4.3 (0.02) ^{Aa}	4.6 (0.01) ^{Ab}	6.4(0.17) ^{Aa}	8.4 (0.17) ^{Ab}	7.1 (0.11) ^{Ba}
IG9									
A/C1	3.8 (0.03)	4.7 (0.02)	5.7 (0.04)	3.8 (0.02)	3.8 (0.01)	4.6 (0.01)	6.2 (0.27)	22.7 (0.32)	19.4 (0.31)
Cd	4.0 (0.02)	5.0 (0.02)	5.7 (0.06)	3.9 (0.02)	4.2 (0.02)	4.4 (0.01)	8.6 (0.23)	9.7 (0.25)	12.5 (0.01)
2A	4.1 (0.04)	4.9 (0.02)	5.4 (0.04)	4.2 (0.02)	4.4 (0.02)	4.7 (0.01)	25.2 (0.14)	23.3 (0.33)	21.5 (0.13)
3C	4.2 (0.02)	-	5.5 (0.02)	4.4 (0.02)	-	4.9 (0.01)	-	16.8 (0.17)	9.2 (0.12)
4B	4.3 (0.03)	4.8 (0.04)	5.1 (0.02)	4.5 (0.02)	4.7 (0.02)	5.0 (0.01)	10.8 (0.28)	12.8 (0.24)	11.3 (0.17)
5C	4.5 (0.01)	4.9 (0.04)	5.1 (0.02)	4.6 (0.01)	5.0 (0.02)	5.3 (0.01)	10.8 (0.23)	0.8 (0.24)	5.1 (0.35)
6C	4.4 (0.03)	5.0 (0.02)	5.3 (0.01)	4.8 (0.02)	5.0 (0.01)	5.4 (0.02)	0.6 (0.17)	0.3 (0.25)	0.5 (0.10)
Mean *	4.2 (0.03) ^{Aa}	4.5 (0.03) ^{Ab}	5.1 (0.03) ^{Ac}	4.4 (0.02) ^{Ba}	4.2 (0.01) ^{Aa}	4.9 (0.01) ^{Bb}	8.4 (0.23) ^{Ba}	9.3 (0.26) ^{Bb}	9.2 (0.17) ^{Ab}

* Depth-weighted average (different uppercase letters express significant difference within the column; different lowercase letters express significant difference within the row; one-way ANOVA, $p < 0.05$).

Table 4. Total organic carbon, total nitrogen, and C/N at different sites (means and standard error).

Sites	Total Organic Carbon (g/kg)			Total Nitrogen (g/kg)			C/N		
	2007	2011	2019	2007	2011	2019	2007	2011	2019
IG7									
A/C1d	-	1.1 (0.1)	3.6 (0.1)	-	0.1 (0.04)	0.5 (0.03)	-	12.4 (0.3)	7.7 (0.5)
C1d	-	1.1 (0.1)	2.2 (0.3)	-	0.1 (0.02)	0.4 (0.03)	-	12.4 (0.6)	5.7 (0.5)
C2d	-	0.8 (0.1)	1.3 (0.1)	-	0.1 (0.02)	0.5 (0.04)	-	11.1 (0.4)	2.8 (0.2)
C3	-	0.8 (0.2)	2.8 (0.1)	-	0.1 (0.02)	0.4 (0.02)	-	11.1 (0.2)	7.5 (0.8)
C4	1.3 (0.2)	1.3 (0.3)	8.0 (0.1)	-	0.1 (0.02)	0.8 (0.01)	-	11.4 (0.2)	10.2 (0.1)
2A1	83.9 (1.6)	96.8 (1.5)	70.6 (1.7)	6.8 (0.1)	7.8 (0.2)	5.8 (0.1)	12.4 (0.5)	12.5 (0.6)	12.2 (0.1)
2A2	46.4 (1.2)	37.5 (1.5)	59.8 (1.1)	3.8 (0.2)	3.3 (0.2)	5.2 (0.2)	12.3 (0.6)	11.4 (0.7)	11.6 (0.1)
2BW	31.0 (1.1)	32.3 (1.2)	31.6 (1.2)	2.6 (0.1)	2.9 (0.1)	2.8 (0.2)	11.8 (0.5)	11.2 (0.2)	11.3 (0.1)
3C	0.6 (0.1)	2.2 (0.3)	4.9 (0.2)	-	0.2 (0.03)	0.7 (0.02)	-	10.9 (0.3)	7.5 (0.2)
Mean *	17.7 (0.8) ^{Aa}	18.7 (0.6) ^{Aa}	20.6 (0.5) ^{Ab}	1.4 (0.1) ^{Aa}	1.5 (0.1) ^{Aa}	1.8 (0.1) ^{Aa}	12.1 (0.5) ^{Aa}	11.4 (0.4) ^{Aa}	9.1 (0.3) ^{Ab}
IG8									
A/C1d	21.9 (1.2)	11.1 (0.1)	38.0 (1.5)	0.9 (0.04)	0.6 (0.04)	2.4 (0.1)	24.5 (1.2)	18.1 (0.7)	15.8 (0.4)
C1d	-	0.4 (0.01)	1.5 (0.4)	-	0.1 (0.03)	0.4 (0.02)	-	5.5 (0.4)	3.9 (0.1)
C2	0.5 (0.01)	0.8 (0.01)	2.3 (0.4)	-	0.1 (0.04)	0.4 (0.01)	-	8.3 (0.1)	5.2 (0.2)
2A	60.5 (1.2)	87.1 (1.2)	69.2 (1.4)	4.2 (0.1)	6.4 (0.1)	5.2 (0.1)	14.6 (0.5)	13.6 (0.6)	13.3 (0.4)
3C	20.1 (1.1)	19.8 (1.1)	36.3 (1.4)	1.4 (0.1)	1.6 (0.1)	2.7 (0.3)	14.5 (0.4)	12.2 (0.5)	13.5 (0.4)
4B	31.8 (1.2)	31.1 (1.1)	22.9 (1.3)	2.2 (0.1)	2.6 (0.1)	1.9 (0.3)	14.2 (0.5)	11.9 (0.7)	12.3 (0.2)
5C	2.8 (0.1)	5.0 (0.1)	3.7 (0.1)	-	0.4 (0.01)	0.5 (0.01)	-	13.2 (0.7)	6.9 (0.2)
Mean *	14.1 (0.8) ^{Ba}	17.2 (0.5) ^{Ab}	16.2 (0.9) ^{Bb}	0.9 (0.1) ^{Ba}	1.3 (0.1) ^{Ab}	1.3 (0.1) ^{Bb}	16.9 (0.7) ^{Ba}	10.8 (0.5) ^{Bb}	8.2 (0.3) ^{Bc}
IG9									
A/C1	-	58.5 (1.4)	47.8 (1.6)	-	4.1 (0.1)	4.1 (0.1)	-	14.2 (0.3)	11.7 (0.3)
Cd	0.2 (0.01)	1.6 (0.4)	11.1 (0.1)	-	0.1 (0.01)	1.2 (0.1)	-	12.0 (0.5)	9.3 (0.6)
2A	76.9 (1.1)	74.1 (1.5)	59.5 (1.4)	6.2 (0.1)	6.6 (0.1)	5.7 (0.1)	12.4 (0.7)	11.2 (0.4)	10.5 (0.1)
3C	20.7 (1.3)	-	44.5 (1.3)	1.7 (0.1)	-	4.0 (0.1)	12.1 (0.3)	-	11.0 (0.1)
4B	30.2 (1.5)	40.6 (1.5)	41.9 (1.4)	2.7 (0.1)	3.7 (0.2)	3.9 (0.3)	11.4 (0.3)	11.1 (0.4)	10.9 (0.2)
5C	7.1 (0.1)	1.6 (0.3)	7.9 (0.1)	0.5 (0.02)	0.1 (0.03)	0.9 (0.02)	14.8 (0.3)	12.5 (0.4)	9.1 (0.1)
6C	-	0.4 (0.02)	1.4 (0.2)	-	0.1 (0.01)	0.3 (0.02)	-	9.0 (0.2)	4.4 (0.2)
Mean *	16.7 (0.8) ^{Aa}	20.2 (0.9) ^{Bb}	24.5 (0.9) ^{Cc}	1.3 (0.1) ^{Aa}	1.7 (0.1) ^{Ab}	2.3 (0.1) ^{Cc}	12.6 (0.4) ^{Aa}	10.3 (0.4) ^{Bb}	8.8 (0.2) ^{Bc}

* Depth-weighted average (different uppercase letters express significant difference within the column; different lowercase letters express significant difference within the row; one-way ANOVA, $p < 0.05$).

Similarly, for the volcanic ash soil accumulated after the volcanic eruption in 2000, the TN content of IG8 was 0.65–0.90 g/kg in 2007, and the TN content of IG7, IG8, and IG9 in 2011 was 0.07–0.09 g/kg, 0.06–0.61 g/kg, and 0.13–4.11 g/kg, respectively. In 2019, the TN content of IG7, IG8, and IG9 was 0.38–0.79 g/kg, 0.38–2.41 g/kg, and 1.19–4.08 g/kg, respectively, and was consistent with the change in the *TOC*. The soil TN also significantly increased with time and decreased with the increase in altitude ($p < 0.05$; Table 4). At the same time, a large amount of soil nitrogen was accumulated in deep soil (Table 4).

The C/N ratio of IG7 in 2007, 2011, and 2019 was 11.81–12.36, 10.91–12.49, and 2.80–12.15, respectively, and the C/N ratio of IG8 was 6.82–24.52, 5.46–18.14, and 3.87–15.78, respectively. The C/N ratio of IG9 was 11.35–12.42, 8.98–14.23, and 4.39–11.73, respectively. The C/N ratio significantly decreased over time ($p < 0.05$; Table 4), and the C/N ratio in the surface horizon was higher, which is consistent with the results of the previous studies, as the C/N ratio of most of the volcanic ash soil profiles decreases with the depth [37–39].

3.7. Evaluation of SQI

The first three principal components explained 85.66% of the total variance (Table 5), and highly weighted indicators were selected from the first three principal components. The highly weighted indicators in the same principal component were significantly correlated with each other, and finally, Total organic carbon (*TOC*), Gas fraction (*GF*), and pH (H_2O) were selected for the calculation of soil quality index (*SQI*). With the weighting values based on PCA, the calculation of *SQI* is given by Equation (3):

$$SQI = 0.62TOC + 0.23GF + 0.15\text{pH} \tag{3}$$

Table 5. Principal component analysis of soil quality indicators.

Principal Component	PC1	PC2	PC3
Eigenvalues	6.94	2.55	1.65
Variance (%)	53.36	19.62	12.68
Bulk density	**−0.96**	−0.16	−0.10
Capillary porosity	**0.93**	−0.22	0.17
Porosity	**0.92**	0.28	0.10
Solid fraction	**−0.92**	−0.28	−0.10
Total nitrogen	**0.90**	0.29	0.08
Total organic carbon	**0.90**	0.30	0.02
Liquid fraction	**0.88**	−0.41	−0.16
Cation exchange capacity	**0.82**	0.20	−0.14
Gas fraction	−0.47	**0.81**	0.31
Non-capillary porosity	−0.34	**0.80**	−0.16
pH (H_2O)	−0.09	−0.47	**0.74**
Hydraulic conductivity	−0.26	0.53	**0.70**
pH (KCl)	0.09	−0.38	**0.62**

Bold factors are considered highly weighted. PC1, PC2, PC3 indicate the first principal component, second principal component, and third principal component, respectively.

Generally, the soil quality index decreased with soil depth and increased with time (Figure 4). In 2019, the surface soil quality index of IG7 was 0.27, which was still lower than that of IG8 and IG9. The buried A horizon still had a higher soil quality index. The classification according to the vegetation type showed that the soil quality index of the surface soil with the highest weathering degree increased gradually with the vegetation succession, and the soil quality index of forest land was much higher than that of grassland (Figure 5).

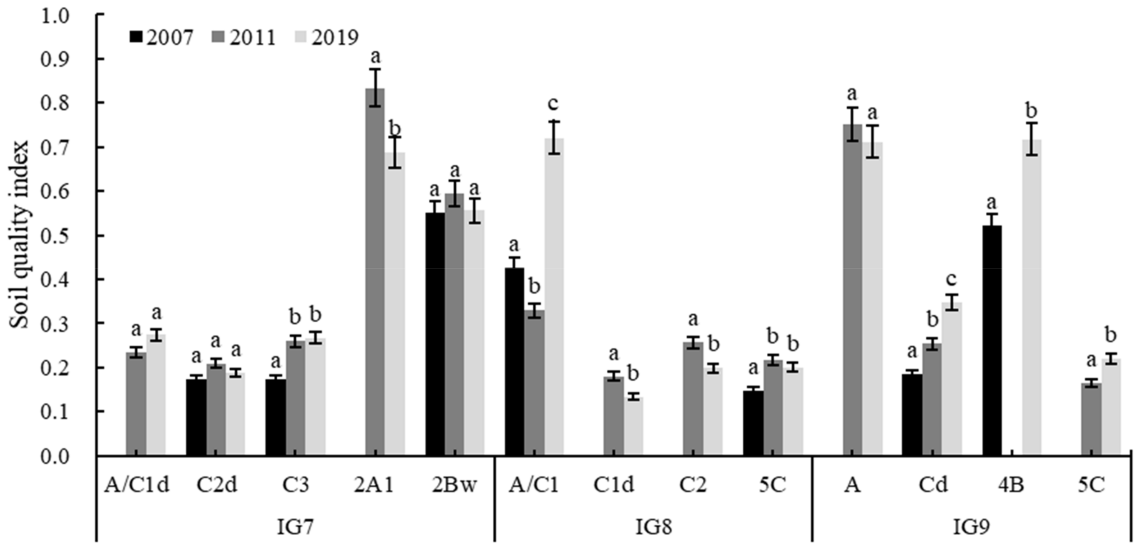

Figure 4. Soil quality index at different sites; different letters express significant difference at the same soil horizon (one-way ANOVA, $p < 0.05$).

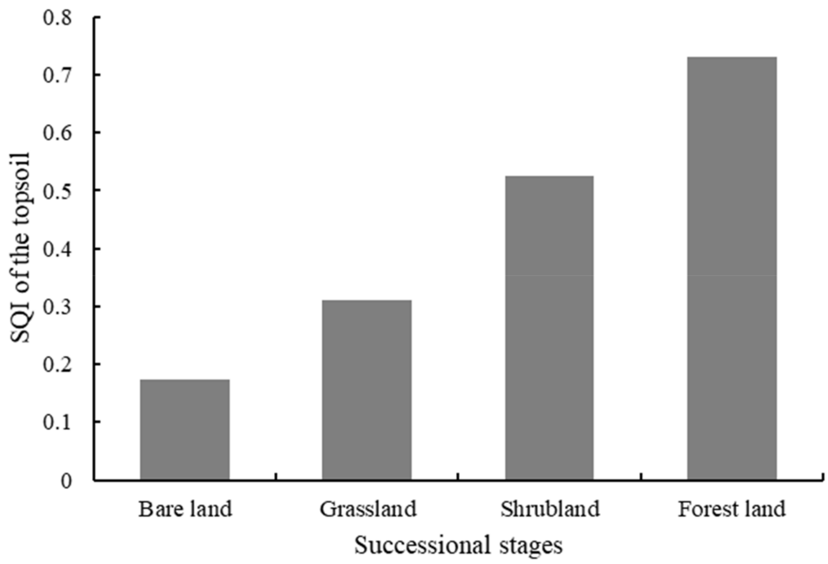

Figure 5. Soil quality index of vegetation types along the successional gradient.

4. Discussion

The soil was formed under the comprehensive actions of climate, vegetation, topography, parent materials, and other factors, and it constantly changed with the vegetation succession. Soil nutrients accumulated continuously with the succession of plant communities, and soil physical properties improved gradually [40]. Different vegetation types lead to differences in root system, litter amount, litter composition, and litter decomposition rate, which leads to differences in soil physical properties [41]. Consistent with previous studies, the vegetation coverage gradually increased over time [42]. In this study, nearly 19 years after the volcanic eruption in 2000, it was found that IG7 was still occupied by herbs (*Miscanthus condensatus*) and that IG8 was covered with herbs (*Miscanthus condensatus*), some shrubs (*Rubus trifidus*), and small nitrogen-fixing trees (*Alnus sieboldiana*), providing strong support for the growth of other plants, as observed in IG9. Before the volcanic eruption, IG9 was a subtropical forest dominated by *Castanopsis sieboldii*, and the colonization of pioneer tree species, such as *Alnus sieboldiana*, could accelerate the succession to the top forest community. Plants affect soil structure and function by promoting microbial activity and the quantity and quality of soil organic matter input [43]. The soil shows a higher mineralization rate of carbon and nitrogen with the vegetation restoration. Many studies have shown that soil function increases with the increase in plant species richness and diversity, such as increasing soil carbon and nitrogen content [44,45], reducing leaching, and improving soil nutrients [46,47]. In this study, the soil quality index increased gradually with the succession from bare land to forest land, which showed the effect of vegetation on soil development. Correspondingly, the plant root system under the soil surface grew from scratch; from less to more, the small gravel gradually disappeared, and the soil surface gradually changed from a hard massive structure to a loose and porous crumb structure. Since Miyake-jima Island is a basaltic stratovolcano with a large amount of calcium in volcanic ash, the calcium was combined with volcanic gas to form hard gypsum (calcium sulfate). In 2007, the surface horizon of IG7 soil was still covered with a hard platy structure with a thickness of 3 cm, which was then replaced in 2019 with an organic horizon with a crumb structure with slightly sticky plastic.

Nearly 19 years after the last volcanic eruption in 2000, IG7 formed a thinner organic horizon, although the soil properties, such as porosity and bulk density, were still lower than those of IG8 and IG9 at low elevations. Unlike IG8 and IG9 covered with shrubs and trees, IG7 was still covered with herbaceous vegetation, showed underdeveloped roots and poor soil permeability. Yu et al. [48] showed that there was a significant positive linear correlation between the soil root density and soil porosity. With the gradual vegetation succession progress, the root system gradually developed, and the improvement effect on the soil bulk density and porosity was gradually strengthened, leading to positive feedback. With the succession of vegetation, the soil bulk density of the IG7, IG8, and IG9 plots gradually decreased, and the soil porosity gradually increased, especially in the surface horizons.

As an important part of soil, soil moisture is related to the transformation and metabolism of matter in the soil, and it plays an important role in the processes of parent material weathering and soil formation. The soil moisture of the IG7, IG8, and IG9 sample plots decreased with the depth, which is consistent with the previous studies. In particular, Miyake-jima Island is an erupting active volcano, and it has an organic horizon with a larger capillary porosity and water content, a relatively loose soil structure in the deep soil horizon, and a water storage capacity stronger than that of other soil horizons on the island. The results of soil porosity showed that IG9 with thinner soil accumulation has looser soil and better water storage capacity. Furthermore, the soil bulk density decreased, and the porosity increased with the vegetation succession, thus increasing the soil hydraulic conductivity. Generally, the soil hydraulic conductivity is related to the soil non-capillary porosity, which is aerated and permeable because it is macroporous, and macropores form macropore flow in the soil, which was proven to be the main factor that determines the soil hydraulic conductivity [49]. Biological macropores (such as root channels) have good connectivity and large pore diameter, which is conducive to the flow of water in soil [50]. In addition, a part of the soil horizon with the large non-capillary porosity, such as the C2d horizon in IG7, had an impact on the hydraulic conductivity due to its massive structure type [51].

With the gradual succession of vegetation growth, the increased amount of litter plays an important role in supplementing soil carbon pools. Furthermore, the biological processes among plants, soil microorganisms, soil animals, as well as abiotic processes, such as the environment and climate, promote the rapid accumulation of surface soil carbon [52,53]. At the same time, with long-term vegetation succession, vegetation cover can fix soil and reduce the losses of soil carbon and nitrogen, which are caused by soil erosion [54]. The soil carbon and nitrogen of the IG7, IG8, and IG9 plots gradually increased with time. Since the IG7 plot, which was near the crater, was still in the herbaceous plant succession stage, the accumulated soil carbon and nitrogen contents were still much lower than those of IG8 and IG9, especially in the surface horizon in which the accumulation of carbon and nitrogen was obvious, even though it increased compared with previous years. Due to the input of organic matter from the roots and root exudates to the deep soil, the carbon and nitrogen contents in the deep soil increased [55], but the growth rate was much lower than that in the surface horizon. Consistent with the results of previous studies, nitrogen limitations generally exist in the processes of soil formation that are accompanied by vegetation successions from the bare lands formed after volcanic eruptions, the C/N ratio gradually decreases with the growth of vegetation, especially in regards to the colonization of nitrogen-fixing plants, and the C/N ratio of most volcanic ash soil profiles decreases with the depth [56]. The soil carbon and nitrogen content are closely related to the physical properties of soil. Sokozoowska et al. [57] showed that the soil enzyme activity and soil microbial content are positively correlated with the soil pore volumes, which can hold air and water. The soil water content and availability can affect the diversity and richness of soil microorganisms, and the decrease in the soil bulk density can promote the survival and development of soil microorganisms. The dynamics of the soil microbial community and the increase in biomass may affect the biogeochemical cycle of soil carbon and other nutrients, resulting in higher carbon sequestrations [58–60].

5. Conclusions

Vegetation succession and the physical and chemical properties of soil influence each other on Miyake-jima Island. Nineteen years after the volcanic eruption, herbaceous vegetation, shrub vegetation, and tree vegetation were formed in high, middle, and low-altitude areas, respectively. The carbon, nitrogen, bulk density, and water holding capacity are the key factors in the succession of the soil's physical and chemical properties. In the process of vegetation growth, the soil bulk density gradually decreased, while the porosity and soil water storage gradually increased. In addition, the soil pH, CEC, and carbon and nitrogen contents further increased, and the change in the soil surface horizon was most obvious. However, the buried horizons of the volcanic ash before the volcanic eruption in 2000 stored a large amount of carbon and nitrogen, and the soil properties were relatively stable. There were some differences in soil covered by different vegetation, and the soil properties of shrubland and forest land were slightly different. However, there was a great difference in the soil properties at the succession stage of the herbaceous communities in the high elevations. The soil quality index (*SQI*) also reflects the same result, and the surface soil quality index at the grassland was still lower than that in shrubland and forest land, and the soil quality index increased gradually with vegetation succession. Under the influence of vegetation, a thinner organic layer was formed 20 years after the volcanic eruption in the high-altitude area, while the organic matter layer was formed in the low-altitude area after 11 years, accumulating more soil carbon and nitrogen than the high-altitude areas.

Supplementary Materials: The following are available online at https://www.mdpi.com/article/10.3390/f12111435/s1, Table S1: Soil profiles morphology of the different research sites, Figure S1: Soil profile photos of the different research sites.

Author Contributions: X.P. and K.T. wrote the manuscript and designed the experiments; A.T. and M.K. edited numerous drafts; M.A. and T.K. revised the manuscript. All authors have read and agreed to the published version of the manuscript.

Funding: This research was funded by KAKENHI, grant number 15H04507, 16H02932, 19H04315, and the Environment Research and Technology Development Fund (Project code D-1106), Ministry of the Environment, Japan.

Data Availability Statement: The data presented in this study are available on request from the corresponding author.

Acknowledgments: We would like to thank Jo Jinno for their extensive support in the fieldwork.

Conflicts of Interest: The authors declare there are no known competing financial interest or personal relationship that could have appeared to influence the work reported in this paper. The funders had no role in the design of the study; in the collection, analyses, or interpretation of data; in the writing of the manuscript, or in the decision to publish the results.

References

1. Vitousek, P.M. The Hawaiian Islands as a model system for ecosystem studies. *Pac. Sci.* **1995**, *49*, 2–16.
2. Oh, N.-H.; Richter, D.D. Elemental translocations and loss from three highly weathered soil-bedrock profiles in the southeastern United States. *Geoderma* **2005**, *126*, 5–25. [CrossRef]
3. Chadwick, O.A.; Chorover, J. The chemistry of pedogenic thresholds. *Geoderma* **2001**, *100*, 321–353. [CrossRef]
4. Riebe, C.S.; Kirchner, J.W.; Finkel, R.C. Sharp decrease in long-term chemical weathering rates along an altitudinal transect. *Earth Planet. Sci. Lett.* **2014**, *218*, 421–434. [CrossRef]
5. White, A.F.; Schulz, M.S.; Stonestrom, D.A.; Vivit, D.V.; Fitzpatrick, J.; Bullen, T.D.; Blum, A.E. Chemical weathering of a marine terrace chronosequence, Santa Cruz, California part II: Solute profiles, gradients and the comparisons of contemporary and long-term weathering rates. *Geochim. Cosmochim. Acta* **2009**, *73*, 2769–2803. [CrossRef]
6. Markewitz, D.; Davidson, E.A.; Figueiredo RD, O.; Victoria, R.L.; Krusche, A.V. Control of cation concentrations in stream waters by surface soil processes in an Amazonian watershed. *Nature* **2001**, *410*, 802–805. [CrossRef]
7. Amundson, R.; Heimsath, A.M.; Owen, J.J.; Yoo, K.; Dietrich, W.E. Hillslope soils and vegetation. *Geomorphology* **2015**, *234*, 122–132. [CrossRef]
8. Chadwick, O.A.; Gavenda, R.T.; Kelly, E.F.; Ziegler, K.; Olson, C.G.; Elliott, W.C.; Hendricks, D.M. The impact of climate on the biogeochemical functioning of volcanic soils. *Chem. Geol.* **2003**, *202*, 195–223. [CrossRef]
9. Lucas, Y. The role of plants in controlling rates and products of weathering: Importance of biological pumping. *Annu. Rev. Earth Planet. Sci.* **2001**, *29*, 135–163. [CrossRef]
10. Viles, H.A. The agency of organic beings: A selective review of recent work in biogeomorphology. In *Vegetation and Erosion: Processes and Environments*; Thornes, J.B., Ed.; Wiley: Chichester, UK, 1990; pp. 5–25.
11. Brantley, S.L.; Lebedeva, M.; Hausrath, E.M. A geobiological view of weathering and erosion. In *Fundamentals of Geobiology*; Knoll, A., Ed.; Wiley-Blackwell: West Sussex, UK, 2012; pp. 205–227. [CrossRef]
12. Drever, J.I. The effect of land plants on weathering rates of silicate minerals. *Geochim. Cosmochim. Acta* **1994**, *58*, 2325–2332. [CrossRef]
13. Dahlgren, R.A.; Saigusa, M.; Ugolini, F.C. The nature, properties and management of volcanic soils. *Adv. Agron.* **2004**, *82*, 113–182. [CrossRef]
14. Jones, G.A.; Henry, G.H.R. Primary plant succession on recently deglaciated terrain in the Canadian High Arctic. *J. Biogeogr.* **2003**, *30*, 277–296. [CrossRef]
15. Leamy, M.L. *Andisols of the World. Congresco International de Suelos Volcanicos, Communicationes, Universida de La Laguna Secretariado de Publicaciones, Serie Informes*; 1984; Volume 13, pp. 368–387.
16. Tsai, C.C.; Chen, Z.S.; Kao, C.I.; Ottner, F.; Kao, S.J.; Zehetner, F. Pedogenic development of volcanic ash soils along a climosequence in northern Taiwan. *Geoderma* **2010**, *156*, 48–59. [CrossRef]
17. Kato, T.; Higashi, T.; Kamijo, T.; Tamura, K. Several chemical and mineralogical properties of volcanic ash samples erupted in 2000 from Miyake Island. *Pedologist* **2002**, *46*, 14–21. (In Japanese) [CrossRef]
18. Kamijo, T.; Kitayama, K.; Sugawara, A.; Urushimichi, S.; Sasai, K. Primary succession of the warm-temperate broad-leaved forest on a volcanic island, Miyake-jima, Japan. *Folia Geobot.* **2002**, *37*, 71–91. [CrossRef]
19. Miyazaki, T. Features of historical eruption at Miyake-jima Volcano. *Bull. Volcanol. Soc. Jpn. Second. Ser. Spec. Issue* **1984**, *29*, S1–S15. (In Japanese) [CrossRef]
20. Nakada, S.; Masashi, N.; Yasuda, A.; Shimano, T.; Nobuo, G.; Marekazu, O.; Toshitsugu, F. Chronology of the Miyakejima. *J. Geogr.* **2001**, *110*, 168–180. (In Japanese) [CrossRef]
21. Yamakoshi, T.; Nakano, M.; Watari, M.; Mizuyama, T.; Chiba, T. Gully development characteristics after the 2000 eruption at Miyakejima Volcano. *J. Jpn. Soc. Eros. Control. Eng.* **2003**, *55*, 40–48. (In Japanese) [CrossRef]
22. Doi, Y.; Yamakoshi, T.; Watari, M. Scoria runoff at Tatsune, Miyakejima island on July 16, 2002. *J. Jpn. Soc. Eros. Control. Eng.* **2003**, *56*, 32–36. (In Japanese) [CrossRef]
23. Kamijo, T. Influence and restoration of vegetation. *J. Jpn. For. Soc.* **2006**, *46*, 46–50. (In Japanese) [CrossRef]
24. Kamijo, T.; Kawagoe, M.; Kato, T.; Kiyohara, Y.; Matsuda, M.; Hashiba, K.; Shimada, K. Destruction and recovery of vegetation caused by the 2000-year eruption on Miyake-jima Island, Japan. *J. Disaster Res.* **2008**, *3*, 226–235. [CrossRef]
25. Takahashi, T.; Kazuhiro, K.; Kamijo, T. The vegetation recovery in Miyakejima Island after the 2000 volcanic eruption using satellite remote sensing. *J. Jpn. Inst. Landsc. Archit.* **2008**, *71*, 539–542. [CrossRef]
26. Ministry of Education—Singapore. *The Third National Survey on the Natural Environment*; Ministry of the Environment: Tokyo, Japan, 1988.
27. Kato, T.; Kamijo, T.; Hatta, T.; Tamura, K.; Higashi, T. Initial Soil Formation Processes of Volcanogenous Regosols (Scoriacious) from Miyake-jima Island, Japan. *Soil Sci. Plant Nutr.* **2005**, *51*, 291–301. [CrossRef]
28. Kottek, M.; Grieser, J.; Beck, C.; Rudolf, B.; Rubel, F. World Map of the Köppen-Geiger climate classification updated. *Meteorol. Z.* **2006**, *15*, 259–263. [CrossRef]
29. Yamanishi, A.; Kamijo, T.; Tsunekawa, A.; Higuchi, H. Monitoring vegetation damage caused by the year 2000 Miyake Island's volcanic eruption using satellite data. *J. Jpn. Inst. Landsc. Archit.* **2003**, *66*, 473–476. [CrossRef]
30. The Japanese Society of Pedology. *The Soil Survey Manual, Revised Edition*; HAKUYUSHA: Tokyo, Japan, 1997.
31. Schollenberger, C.J.; Simon, R.H. Determination of exchange capacity and exchangeable bases in soil. Ammonium acetate method. *Soil Sci.* **1945**, *59*, 13–24. [CrossRef]

32. Andrews, S.S.; Mitchell, J.P.; Mancinelli, R.; Karlen, D.L.; Hartz, T.K.; Horwath, W.R.; Pettygrove, G.S.; Scow, K.M.; Munk, D.S. On-farm assessment of soil quality in California's Central Valley. *Agron. J.* **2002**, *94*, 12–23. [CrossRef]
33. Masto, R.E.; Chhonkar, P.K.; Singh, D.; Patra, A.K. Alternative soil quality indices for evaluating the effect of intensive cropping, fertilisation and manuring for 31 years in the semi-arid soils of India. *Environ. Monit. Assess.* **2008**, *136*, 419–435. [CrossRef] [PubMed]
34. Bastida, F.; Moreno, J.L.; Hernandez, T.; Garcia, C. Microbiological degradation index of soils in a semiarid climate. *Soil Biol. Biochem.* **2006**, *38*, 3463–3473. [CrossRef]
35. Zhao, K.; Fahey, T.J.; Liang, D.; Jia, Z.; Ma, L. Effects of long-term successive rotations, clear-cutting and stand age of prince Rupprecht's larch (Larix principis-rupprechtii Mayr) on soil quality. *Forests* **2019**, *10*, 932. [CrossRef]
36. Li, D.; Si, J.; Zhang, X.; Gao, Y.; Luo, H.; Qin, J.; Gao, G. The mechanism of changes in hydraulic properties of Populus euphratica in response to drought stress. *Forests* **2019**, *10*, 904. [CrossRef]
37. Arnold, J.; Corre, M.D.; Veldkamp, E. Soil N cycling in old-growth forests across an andosol toposequence in Ecuador. *For. Ecol. Manag.* **2009**, *257*, 2079–2087. [CrossRef]
38. Peña-Ramírez, V.M.; Vázquez-Selem, L.; Siebe, C. Soil organic carbon stocks and forest productivity in volcanic ash soils of different age (1835–30,500 years B.P.) in Mexico. *Geoderma* **2009**, *149*, 224–234. [CrossRef]
39. Molina, A.; Vanacker, V.; Corre, M.D.; Veldkamp, E. Patterns in soil chemical weathering related to topographic gradients and vegetation structure in a high Andean tropical ecosystem. *J. Geophys. Res. Earth Surf.* **2019**, *124*, 666–685. [CrossRef]
40. Kang, B.; Liu, S.R.; Cai, D.X.; Lu, L.H.; He, R.M.; Gao, Y.X.; Di, W.Z. Soil physical and chemical characteristics under different vegetation restoration patterns in China south subtropical area. *Ying Yong Sheng Tai Xue Bao J. Appl. Ecol.* **2010**, *21*, 2479–2486.
41. Miao, R.H.; Song, Y.H.; Sun, Z.L.; Guo, M.X.; Zhou, Z.X.; Liu, Y.Z. Soil seed bank and plant community development in passive restoration of degraded sandy grasslands. *Sustainability* **2016**, *8*, 581. [CrossRef]
42. Bach, E.M.; Baer, S.G.; Six, J. Plant and soil responses to high and low diversity grassland restoration practices. *Environ. Manag.* **2012**, *49*, 412–424. [CrossRef]
43. Cardinale, B.J.; Duffy, J.E.; Gonzalez, A.; Hooper, D.U.; Perrings, C.; Venail, P.; Narwani, A.; Mace, G.M.; Tilman, D.; Wardle, D.A.; et al. Biodiversity loss and its impact on humanity. *Nature* **2012**, *486*, 59–67. [CrossRef]
44. Tahmasebi, P.; Moradi, M.; Omidipour, R. Plant functional identity as the predictor of carbon storage in semi-arid ecosystems. *Plant Ecol. Divers.* **2017**, *10*, 139–151. [CrossRef]
45. Tilman, D.; Reich, P.B.; Knops, J.M. Biodiversity and ecosystem stability in a decade-long grassland experiment. *Nature* **2006**, *441*, 629–632. [CrossRef]
46. Dijkstra, F.A.; West, J.B.; Hobbie, S.E.; Reich, P.B.; Trost, J. Plant diversity, CO_2, and N influence inorganic and organic N leaching in grasslands. *Ecology* **2007**, *88*, 490–500. [CrossRef]
47. Li, D.S.; Zhang, P.; Zhang, S.L.; Yin, J.D.; Lu, F.D. A study on water conservation capacity of forest soil in Huangqian reservoir area. *J. Nanjing For. Univ.* **2004**, *28*, 25–27.
48. Yu, B.; Xie, C.; Cai, S.; Chen, Y.; Lv, Y.; Mo, Z.; Yang, Z. Effects of tree root density on soil total porosity and non-capillary porosity using a ground-penetrating tree radar Unit in Shanghai, China. *Sustainability* **2018**, *10*, 4640. [CrossRef]
49. Ahuja, L.R.; Naney, J.W.; Green, R.E.; Nielsen, D.R. Macroporosity to characterize spatial variability of hydraulic conductivity and effects of land management. *Soil Sci. Soc. Am. J.* **1984**, *48*, 699–702. [CrossRef]
50. Ajayi, A.E.; Horn, R. Transformation of ex-arable land to permanent grassland promotes pore rigidity and mechanical soil resilience. *Ecol. Eng.* **2016**, *94*, 592–598. [CrossRef]
51. Gu, C.; Mu, X.; Gao, P.; Zhao, G.; Sun, W.; Tatarko, J.; Tan, X. Influence of vegetation restoration on soil physical properties in the loess plateau, china. *J. Soils Sediments* **2019**, *19*, 716–728. [CrossRef]
52. Hooper, D.U.; Bignell, D.E.; Brown, V.K.; Brussard, L.; Mark Dangerfield, J.; Wall, D.H.; Wardle, D.A.; Coleman, D.C.; Giller, K.E.; Lavelle, P.; et al. Interactions between aboveground and belowground biodiversity in terrestrial ecosystems: Patterns, mechanisms and feedbacks. *BioScience* **2000**, *50*, 1049–1061. [CrossRef]
53. Tang, X.Y.; Liu, S.G.; Liu, J.X.; Zhou, G.Y. Effects of vegetation restoration and slope positions on soil aggregation and soil carbon accumulation on heavily eroded tropical land of Southern China. *J. Soils Sediments* **2010**, *10*, 505–513. [CrossRef]
54. Fu, X.L.; Shao, M.A.; Wei, X.R.; Horton, R. Soil organic carbon and total nitrogen as affected by vegetation types in Northern Loess Plateau of China. *Geoderma* **2010**, *155*, 31–35. [CrossRef]
55. Nelson, J.D.J.; Schoenau, J.J.; Malhi, S.S. Soil organic carbon changes and distribution in cultivated and restored grassland soils in Saskatchewan. *Nutr. Cycl. Agroecosystems* **2008**, *82*, 137–148. [CrossRef]
56. Gamboa, A.M.; Galicia, L. Land-use/cover change effects and carbon controls on volcanic soil profiles in highland temperate forests. *Geoderma* **2012**, *170*, 390–402. [CrossRef]
57. Sokołowska, J.; Józefowska, A.; Woźnica, K.; Zaleski, T. Succession from meadow to mature forest: Impacts on soil biological, chemical and physical properties—Evidence from the Pieniny mountains, Poland. *CATENA* **2020**, *189*, 104503. [CrossRef]
58. Cleveland, C.C.; Townsend, A.R.; Constance, B.C.; Ley, R.E.; Schmidt, S.K. Soil microbial dynamics in Costa Rica: Seasonal and biogeochemical constraints. *Biotropica* **2004**, *36*, 184–195. [CrossRef]
59. Li, Y.Y.; Shao, M.A.; Zheng, J.Y.; Zhang, X.C. Spatial-temporal changes of soil organic carbon during vegetation recovery at Ziwuling, China. *Pedosphere* **2005**, *15*, 601–610.
60. Deng, L.; Wang, K.; Chen, M.; Shangguan, Z.; Sweeney, S. Soil organic carbon storage capacity positively related to forest succession on the loess plateau, China. *CATENA* **2013**, *110*, 1–7. [CrossRef]